MAGNETIC RESONANCE IN CHEMISTRY
Magn. Reson. Chem. 2007; **45**: S2–S11
Published online 19 December 2007 in Wiley InterScience
(www.interscience.wiley.com) DOI: 10.1002/mrc.2077

MRC

Review

Lipid bilayers: an essential environment for the understanding of membrane proteins

Richard C. Page,[1,2] Conggang Li,[1,2] Jian Hu,[1,2] Fei Philip Gao[1,2] and Timothy A. Cross[1,2]*

[1] Department of Chemistry and Biochemistry, Florida State University, Tallahassee, FL 32306-4390, USA
[2] National High Magnetic Field Laboratory, 1800 E. Paul Dirac Drive, Tallahassee, FL 32310, USA

Received 15 June 2007; Revised 20 July 2007; Accepted 6 August 2007

Membrane protein structure and function is critically dependent on the surrounding environment. Consequently, utilizing a membrane mimetic that adequately models the native membrane environment is essential. A range of membrane mimetics are available but none generates a better model of native aqueous, interfacial, and hydrocarbon core environments than synthetic lipid bilayers. Transmembrane α-helices are very stable in lipid bilayers because of the low water content and low dielectric environment within the bilayer hydrocarbon core that strengthens intrahelical hydrogen bonds and hinders structural rearrangements within the transmembrane helices. Recent evidence from solid-state NMR spectroscopy illustrates that transmembrane α-helices, both in peptides and full-length proteins, appear to be highly uniform based on the observation of resonance patterns in PISEMA spectra. Here, we quantitate for the first time through simulations what we mean by highly uniform structures. Indeed, helices in transmembrane peptides appear to have backbone torsion angles that are uniform within ±4°. While individual helices can be structurally stable due to intrahelical hydrogen bonds, interhelical interactions within helical bundles can be weak and nonspecific, resulting in multiple packing arrangements. Some helical bundles have the capacity through their amino acid composition for hydrogen bonding and electrostatic interactions to stabilize the interhelical conformations and solid-state NMR data is shown here for both of these situations. Solid-state NMR spectroscopy is unique among the techniques capable of determining three-dimensional structures of proteins in that it provides the ability to characterize structurally the membrane proteins at very high resolution in liquid crystalline lipid bilayers. Copyright © 2007 John Wiley & Sons, Ltd.

KEYWORDS: NMR; ^{1}H; ^{15}N; integral membrane proteins; PISEMA; sample preparation; oriented lipid bilayers

INTRODUCTION

Many obstacles have conspired to impede the detailed biophysical characterization of membrane proteins, but none of them are more significant than the challenge of providing an adequate model of the membrane protein environment for these studies. The structure, dynamics, and function of membrane proteins are all influenced by this environment and consequently, it is essential that membrane proteins are characterized in a native-like environment. Typically, crystallography and solution NMR utilize a detergent environment as a model membrane mimetic environment and while this models certain aspects of the native membrane it is not as good a model as a lipid bilayer. Unlike the aqueous environment for water-soluble proteins, the membrane environment is very complex and heterogeneous. Solid-state NMR spectroscopy provides a unique ability to characterize membrane proteins not only in a lipid bilayer, but also in a lipid bilayer above the gel to liquid crystalline phase transition temperature.

*Correspondence to: Timothy A. Cross, National High Magnetic Field Laboratory, 1800 E. Paul Dirac Drive, Tallahassee, FL 32310, USA. E-mail: cross@magnet.fsu.edu

Membrane proteins and the lipid bilayer environment

The numerous membranes of living cells are composed of a heterogeneous array of lipids, proteins and other membrane-soluble components. Membranes can be compartmentalized as has been discussed extensively in the recent 'lipid raft' literature.[1] Membranes form barriers between two aqueous compartments where the interior of the membrane is essentially devoid of water. Not only is there a steep water concentration gradient, but also gradients in dielectric constant,[2] molecular dynamics[3] and in lateral pressure.[2,4] The anisotropy of lipid bilayers is used by cells to generate vital electrical, chemical, and mechanical potentials, which are derived from or lead to phenomena, such as membrane thinning, hydrophobic mismatch, curvature frustration, charge polarization, and lateral force gradients.[5,6] These phenomena affect membrane protein structure, orientation, dynamics, and function. One of the results is that the delicate balance of forces that accounts for protein structural

stability is very different for membrane proteins than for water-soluble proteins. Membrane mimetic environments that range from organic solvents to synthetic lipid bilayers model some of these properties, but not all of them. Detergent micelles provide good approximations of the local aqueous, interfacial, and hydrocarbon core regions of native bilayers, yet they are poor at reproducing native membrane curvature, lateral pressure profiles, and water content. Organic solvent mixtures (mixed polarity solvents) can reasonably approximate the bilayer hydrocarbon core, but are extremely poor mimetics of interfacial and aqueous regions and offer no opportunity for reproducing lateral pressure, membrane curvature, and water concentration gradients. However, synthetic lipid bilayers can provide aqueous, interfacial, and hydrocarbon core environments that are nearly identical to those found in native lipid bilayers. Furthermore, only synthetic lipid bilayers allow for the controlled variation of membrane lipid composition enabling essential studies of membrane protein structure and function in environments with differing lateral pressures, hydrophobic thicknesses or membrane curvatures. Synthetic lipid bilayers clearly generate the most native-like environment that can be used for three-dimensional structure determination.

Membrane proteins are fundamentally very different from water-soluble proteins. The amino acid composition of these proteins in the transmembrane domain (TMD) is significantly different from that of water-soluble proteins[7] (Fig. 1). Charged residues (Arg, Lys, Asp, Glu, and His) are more common in water-soluble α-helices than transmembrane (TM) α-helices by nearly a factor of three. The same factor applies to the amide side-chain residues. The hydrophobic and weakly hydrophilic residues (Val, Leu, Ile, Met, Phe, Gly, Ser, Thr, and Trp) are more common in membrane proteins than water-soluble proteins by 50%. This radically different composition reflects the very different environments for these two classes of proteins.

For many membrane proteins, the largely greasy interface between TM helices, dictated by the predominantly hydrophobic amino acid composition, is dominated by van der Waals interactions and other weak, relatively nonspecific electrostatic interactions. Hydrogen bonding is site-specific, but for many TM helix–helix interfaces hydrogen bonding is rare, again because of the amino acid composition. When van der Waals interactions dominate the helix–helix interface, it is anticipated that the nonspecificity of these interactions will permit dynamics between helices and permit multiple low energy interacting states.[6] There is a large literature that documents almost indiscriminate chemical cross-linking between helices in polytopic membrane proteins provided the reaction times are lengthy.[8] These results strongly support the hypothesis of conformational flexibility at these hydrophobic helix–helix interfaces. Recently, hydrogen–deuterium exchange in a 44 kDa tetrameric membrane protein complex has shown through solid-state NMR that rotational excursions occur about the helical axis exposing the normally lipid facing amides to the aqueous pore.[9] Loops between helices and between β-strands have also been shown in some cases to be highly dynamic, thereby

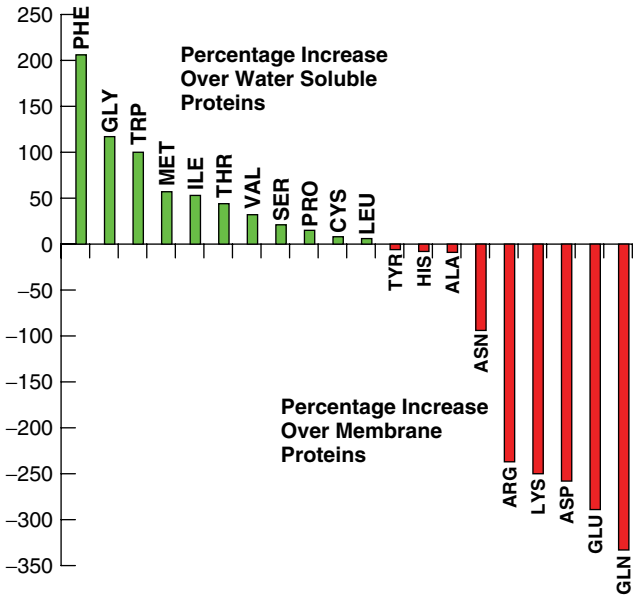

Figure 1. Comparison of amino acid compositions in transmembrane (TM) regions of α-helical membrane proteins *versus* water-soluble proteins. For those amino acids that are more common in membrane proteins (green), the data represents the % increase over that found in water-soluble proteins. For those amino acids that are more common in water-soluble proteins (red), the data represents the % increase over that found in membrane proteins (adapted from Eilers *et al*., 2002)[7].

permitting such motions.[10,11] Furthermore, it is well recognized for membrane proteins that multiple functional states involve different packing arrangements of α-helices.[12] For membrane proteins that do not have interhelical hydrogen bonding, the potential for interhelical dynamics and structural heterogeneity represents a major departure from the water-soluble proteins that are most readily characterized by solution NMR and X-ray crystallography. However, helix–helix interactions can, on occasion, be quite strong in membrane proteins; glycophorin is now a classic example of a coiled-coil helical pair with the GxxxG sequence motif.[13,14]

The lipid bilayer is an environment that can readily trap nonminimum energy conformations[15] and owing to the low water content, hydrogen bond rearrangements in membrane proteins are much less common than for water-soluble proteins. In part, the lack of water in the membrane interior and the necessity for water in folding α-helices explains why membrane proteins are largely folded at the membrane interface (in presence of water) prior to transmembrane insertion.[16–18] In this process, the intrahelical hydrogen bonds are formed prior to insertion of the helix across the membrane. Water is a catalyst for hydrogen bond rearrangements in the nonpolar interior of the lipid bilayer in that it destabilizes intramolecular hydrogen bonds and stabilizes broken hydrogen bond intermediates.[19–22] However, aqueous access to the amide backbone in membrane proteins is quite variable; while most of the amide protons of lac permease can be readily exchanged,[23] the amides in the TM region of diacylglycerol kinase are extremely resistant to H–D exchange.[24]

DOI: 10.1002/mrc

NMR spectroscopy for membrane proteins

NMR spectroscopy permits detailed structural and dynamic characterizations in a variety of membrane mimetic environments. X-ray crystallography has been very helpful in providing most of the current membrane protein structures in the Protein Data Bank, but most of these structures are large oligomeric structures with a high ratio of molecular volume to hydrophobic surface area. While NMR methods are complementary to crystallographic methods, they are more appropriate for smaller membrane proteins with a proportionately large hydrophobic surface area. In the *Mycobacterium tuberculosis* (*Mtb*) genome, more than 70% of all membrane proteins have a monomeric molecular weight <45 kDa. Solution NMR can provide high-resolution information, yet it is currently limited to membrane proteins with a total oligomeric weight on this order due to increased relaxation rates for increasingly larger protein–detergent micelle complexes. For solid-state NMR using aligned samples or magic angle spinning samples, there is no such relaxation induced limitation on the size of membrane proteins, but rather a current practical limitation based on resonance resolution in the two- and three-dimensional spectra represented by a similar molecular weight. However, if the protein is oligomeric with an axis of symmetry this limitation applies only to the monomer molecular weight and not to the molecular weight of the oligomer.

For solid-state NMR samples, it is possible to modify the membrane protein's environment. Not only can lipids be changed, but changes to the salt concentration, pH or various other additives to the aqueous or lipid (detergent) environment can also be made. For packed liposomes used in magic angle sample spinners, it is relatively easy to change sample conditions, while alignment of planar bilayers between glass slides represent a considerable impediment for changing the solvent environment. Aligned samples in anodic aluminum oxide (AAO) nanoporous membranes provides an opportunity to change the sample conditions even while the sample remains in the NMR probe.[25] While complete structural characterization may not be possible for all the ranges of environmental conditions, it is still possible to monitor sites within the protein for changes in structure, dynamics or chemical environment. Such high-resolution monitoring (observation of specific amino acid sites) of chemical environments is not possible by any other approach that also has the potential to characterize three-dimensional structures of membrane proteins.

Sample preparation is critically important for all structural methodologies. Here, for solid-state NMR the preparation of oriented lipid bilayer samples is routine for helical TM peptides, but the alignment of full-length membrane proteins has been challenging for some cases. In addition, heating of oriented lipid bilayer samples by high power radio frequency irradiation used during NMR experiments has generated heterogeneous samples.[26] This latter problem has been elegantly solved with the development of low-electric field probes[27] and the former problem is fading as we begin to understand that some proteins (maybe quite a few monotopic proteins) are designed to distort the planarity of lipid bilayers or to take advantage of nonplanar membranes.

Here, the solid-state NMR experiments utilize the polarization inversion spin exchange at the magic angle (PISEMA) pulse sequence[28] that correlate anisotropic ^{15}N chemical shifts and ^{15}N–^{1}H dipolar couplings from the polypeptide backbone.[29] Resonance patterns, known as polarity index slant angle (PISA) wheels, can be observed in spectra of TM helices representing an image of the helix[30,31] and based on the size, shape, and position of the PISA wheel, the tilt angle of the helix axis with respect to the bilayer normal can be determined with considerable accuracy (Fig. 2). The observation of these patterns can be used to provide considerable additional biophysical information about membrane proteins and the energetics of helices formed in this environment that makes them so different from helices in water-soluble proteins.

MATERIALS AND METHODS

Oriented bilayer samples

Solid-State NMR samples consisted of either TM peptides or full-length membrane proteins incorporated into oriented lipid bilayers aligned on glass slides. Unless otherwise noted, all samples were prepared with lipid bilayers composed of 1,2-dimyristoyl-*sn*-glycero-3-phosphocholine (DMPC) and 1,2-dimyristoyl-*sn*-glycero-3-[phospho-*rac*-(1-glycerol)] (DMPG) mixed in a 4 : 1 (DMPC : DMPG) molar ratio. Other lipids used to prepare oriented bilayer samples include 1,2-dilauroyl-*sn*-glycero-3-phosphocholine (DLPC), 1-palmitoyl-2-oleoyl-*sn*-glycero-3-phosphocholine (POPC), 1-palmitoyl-2-oleoyl-*sn*-glycero-3-[phospho-*rac*-(1-glycerol)] (POPG), 1,2-dioleoyl-*sn*-glycero-3-phosphocholine (DOPC), 1,2-dioleoyl-*sn*-glycero-3-[phospho-*rac*-(1-glycerol)] (DOPG), and *Escherichia coli* total lipid extract (*E. coli* lipid). All lipids were purchased from Avanti Polar Lipids, Inc. (Alabaster, AL). Peptide and full-length protein samples were prepared with a 10 : 1 (w : w) ratio of lipid to protein. Samples of TM peptides were prepared either by detergent mediated reconstitution[9,32] or organic solvent reconstitution.[33,34] Full-length protein samples were prepared exclusively via detergent mediated reconstitution.

Samples prepared via detergent mediated reconstitution began with peptides or proteins solubilized in either n-Octyl-β-D-glucoside (OG) or sodium dodecyl sulfate (SDS). Lipids

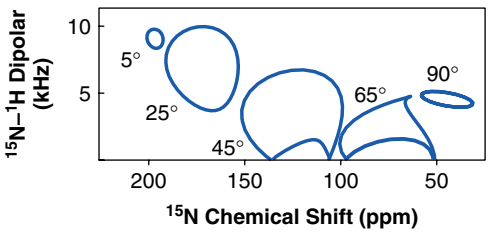

Figure 2. Resonances within PISEMA spectra form characteristic patterns called PISA wheels. Here, PISA wheels are displayed for helices with helix axis tilt angles (τ) of 5°, 25°, 45°, 65°, and 90° with respect to the bilayer normal. Like helical wheels, 3.6 resonances per turn around the PISA wheel are observed. This set of patterns is for oriented lipid bilayer samples aligned on glass slides with the bilayer normal parallel to the magnetic field.

DOI: 10.1002/mrc

were introduced either as preformed liposomes or dry lipid powder. Preformed liposomes were prepared by dissolving lipids in a mixture of chloroform and methanol (1 : 1) in a round bottom flask, removing the solvent by rotary evaporation, drying overnight under vacuum, resuspension of the lipid film in warm (37 °C) deionized water; bath sonication of resuspended lipids and three repetitions of freeze-thaw cycling followed ultimately by dilution to 20 mg/ml. For addition of either preformed liposomes or lipid powder, samples were thoroughly yet gently mixed yielding a viscous, semi-transparent protein–lipid–detergent mixture. A solution of 20% detergent (either OG or SDS) was added in 100 µl aliquots with gentle mixing until the solution became transparent and the viscosity was similar to that of an aqueous solution. Detergent was removed via exhaustive dialysis against deionized water. Following dialysis, proteoliposomes were pelleted via ultracentrifugation at 90 000 × g for 3 h.

Samples prepared via organic solvent reconstitution began with lyophilized peptides dissolved in 1 ml methanol. Lipids solubilized in 2 ml methanol : trifluoroethanol (1 : 1) were added to methanol solubilized peptides and thoroughly mixed with swirling and vortexing. Peptide–lipid mixtures were dried to a film under a N_2 gas stream followed by drying overnight under vacuum. Dried peptide–lipid films were gently resuspended in warm (37 °C) 10 mM borate–potassium chloride–sodium hydroxide buffer; pH 9. Resuspended peptide–lipid films were incubated with gentle shaking at 37 °C overnight followed by dialysis against 10 mM borate–potassium chloride–sodium hydroxide buffer; pH 9. After overnight dialysis, proteoliposomes were pelleted via ultracentrifugation at 90 000 × g for 3 h.

Regardless of the reconstitution method used to produce proteoliposome pellets, the final plating steps for preparation of oriented lipid bilayer samples on glass slides were identical for all the samples. Pelleted proteoliposomes were gently resuspended in HPLC-grade water to a final volume of approximately 1.5 ml. Resuspended proteoliposomes were briefly sonicated to ensure a homogeneous suspension. Aliquots of resuspended proteoliposomes were spread onto 30 to 40 glass slides (12 × 7 × 0.07 mm, Paul Marienfeld GmbH & Co.), dried for 2 h at room temperature, stacked and inserted into a rectangular glass sample cell (NE-RSC-4.3 × 6.3 – 20-FB, New Era Inc.). Samples were rehydrated by incubation at 98% relative humidity for at least 7 days at 37 °C (above the gel to liquid crystalline phase transition temperature). Rehydrated samples were sealed with wax and used for solid-state NMR experiments.

Acquisition of PISEMA spectra

All PISEMA spectra were acquired at 600 MHz utilizing NHMFL low-E probes[27] with the exception of the KdpF spectrum that was acquired on the Ultra Wide Bore 900 MHz spectrometer at the NHMFL. All PISEMA spectra used the following parameters: 800 µs cross-polarization contact time, 4 ms acquisition time, 6 s recycle delay, and ^{1}H decoupling with the SPINAL scheme.[35] Spectra were typically acquired with 32 t_1 increments resulting in total acquisition times ranging from 6 h to 3 days. All experiments were conducted at either 30 or 40 °C; well above the gel to liquid crystalline phase transition for the bilayer systems employed. Spectra were processed using in-house scripts written for NMRPipe.[36] Processing scripts included the following: zero filling of t_2 to 1024 points, linear prediction of t_1 to 128 points; exponential multiplication window function for t_1 and t_2 domains with 164 Hz Lorentzian line broadening to enhance signal to noise; shifted sine bell curve for both t_1 and t_2 domains; Lorentz-to-Gauss window function to reduce linewidths; Fourier transformation of both t_1 and t_2 time domains; correction of the ^{15}N–^{1}H-dipolar coupling dimension by a scaling factor of 0.816 (sin 54.7°). ^{15}N-chemical shifts were referenced to liquid ammonia at 0 ppm via a saturated solution of $^{15}NH_4NO_3$ at 26 ppm. All spectra were plotted using Sparky[37] with $\nu = (0, 12\ \text{kHz})$, $\sigma = (92\,238\ \text{ppm})$ for TM peptides and $\nu = (0, 12\ \text{kHz})$, $\sigma = (26\,238\ \text{ppm})$ for full-length membrane proteins.

PISEMA spectra simulations

Simulated PISEMA spectra, PISA wheels and Ramachandran plots were calculated using in-house scripts written for MatLab (The MathWorks, Inc.). PISEMA spectra were simulated for an 18-residue α-helix with 0° rotation about the helical axis ($\rho = 0°$) while the helix axis tilt angle (τ) and backbone torsion angles (ϕ,ψ) were allowed to vary, as indicated. Randomized variations in (ϕ, ψ) about the idealized values ($\phi = -60°$, $\psi = -45°$)[38] for each residue were generated using a random number generator within MatLab. Simulations utilizing randomized backbone torsion angle variations are denoted as ϕ, $\psi = \pm x°$, where x is the upper and lower limit of sampling space for the randomized number generator. For example, a randomized variation of $x = 2°$ generates torsion angles in the range of $\phi = -58$ to $-62°$ and $\psi = -43$ to $-47°$. Both the motionally-averaged chemical shift tensor ($\sigma_{11} = 57.3$, $\sigma_{22} = 81.2$, $\sigma_{33} = 227.8$ ppm) and motionally-averaged dipolar magnitude ($\nu = 10.735$ kHz) were held constant throughout all the simulations based on experimental data.[30] The relative orientation (θ) between the chemical shift tensor element σ_{33} and $\nu_{||}$ of the dipolar tensor was set to 17°, consistent with previous simulations[30] and experiments.[39] All ^{15}N-chemical shifts were referenced as described above for NMR data acquisition.

RESULTS AND DISCUSSION

Amino acid composition in TM helices

The amino acid composition of TM helices has been discussed extensively in the literature[7] where it has been documented that the hydrophobic content is dramatically elevated and charged residues are much more rare in comparison to helices in water-soluble proteins. On the basis of the propensity for certain residues to be buried in the membrane interstices, a great deal of work has been done on hydrophobicity scales[40,41] and probabilities for finding residues at different depths within the bilayer.[42] Tryptophan is most commonly found at the aqueous–fatty acid interface as are tyrosine, lysine, and arginine. Each of these residues have hydrophobic and hydrophilic regions that facilitate the partitioning of the

DOI: 10.1002/mrc

residue at this membrane interface. Glycine and proline are known to be helix breakers based on our knowledge of water-soluble proteins, but they are very commonly found in the middle of TM helical sequences. Apparently, the potential that these residues exert on the helix is not large enough to destabilize helices in the TM environment.

Figure 3 displays the amino acid sequences of the peptides and proteins discussed in this paper. The amino acid composition and distribution, in general, follows that which has been illustrated in the literature. CorA is a Mg^{2+} transporter obtained from *Mtb*. Its structure has recently been solved as displaying ten TM helices that form a pentameric structure.[43] The interhelical periplasmic loop with highly conserved sequences was unresolved in the crystal structure. Here, only a peptide named CorA-TM2 corresponding with residues 336–366 is characterized. KdpC, also from *Mtb*, is a component of the K^+ transporting Kdp complex having a single TM helix and a large water-soluble *C*-terminal domain.[44] Rv1861 is another *Mtb* membrane protein with no known function. It has three TM helices and forms an octameric state.[45] M2 protein from Influenza A is a well known drug target and its TMD has been structurally characterized with[46] and without[47] the antiviral drug amantadine. Diacylglycerol kinase (DAGK) from *E. coli* has been modified to increase the stability of the trimeric structure[24,48] with three mutations – I53C, I70L and V107D. DAGK has three TM helices.

TM helix structure in lipid bilayers

Due to the low dielectric environment in the TM region, electrostatic interactions, when present, are greatly strengthened relative to such interactions in a much higher dielectric environment. Hydrogen bonds, when formed, are not likely to rearrange bonding partners because of the increased strength of these interactions. This phenomenon has been observed both by X-ray crystallography[49] and by solid-state

```
CorA-TMD  307-  RKISAWAGII AVPTMIAGIY GMNFHFMPEL DSRWGYPTVI
                GGMVLICLFL YHVFRNRNWL
KdpC-TMD    1-  MRRQLLPALT MLLVFTVITG IVYPLAVTGVG
Rv1861      1-  MDITATTEFS AMNLDGKTGI GWLGYIVIGG IAGWLASKIV
                KGGGSGILMN VVIGVVGAFG AGLVLNALGV DVNHGGYWFT
                FFVALGGAVV LLWIVGMVRK T
KdpF        1-  MTTVDNIVGL VIAVALMAFL FAALLFPEKF
M2-TMD     22-  SSDPLVVAAS IIGILHLILW ILDRL
DAGK        1-  ANNTTGFTRI IKAAGYSWKG LRAAWINEAA FRQEGVAVLL
                AVVIACWLDV DACTRVLLIS SVMLVMIVEL LNSAIEAVVD
                RIGSEYHELS GRAKDMGSAA VLIAIIDAVI TWCILLWSHF
                G
```

Figure 3. The amino acid sequences for proteins and peptides used for this study are presented. The putative transmembrane (TM) sequences are highlighted in yellow. The glycine and proline residues in these TM regions are shown in green and charged resonances are shown for the entire sequences in red. While the amino acid composition of the TMDs for CorA, DAGK, KdpC, KdpF, and M2 are predominantly hydrophobic, polar and charged residues are occasionally tolerated towards the ends of TM helices and glycine and proline residues often do not break the helical structure as they do in water-soluble proteins.

NMR[38] through the characterization of short α-helical hydrogen bonds in the membrane environment where there is a vastly reduced frequency of multiple hydrogen bonds to backbone helical carbonyl oxygens.[50] In addition, water which, if present, would act as a catalyst for hydrogen bond rearrangements[22] by destabilizing hydrogen bonds and stabilizing the N–H and C=O intermediates in such a rearrangement, but this is very scarce in membrane interstices. Therefore, once formed, helices are not likely to rearrange hydrogen-bonding patterns. Indeed, this may result in kinetically trapped conformations.[15] The environmental stabilization of helical structure appears to be an explanation for the frequent occurrence of glycine and proline residues in TM helices. The PISEMA spectra in Fig. 4 of the CorA-TM2 and M2-TMD peptides show uniform helical structures despite the presence of glycine residues in the very middle of these sequences.

Numerous peptides have been aligned in planar bilayers in our lab,[46,47,51] some of which are represented here, and many others have been aligned in other labs also using planar bilayers,[52–55] bicelles[56–58] or aligned samples in AAO nanotubes.[59,60] All the spectra presented in Fig. 4 are from planar bilayer preparations. The PISEMA spectra in Fig. 4 of each uniformly aligned lipid bilayer-bound peptide sample show a pattern of resonances, known as PISA wheels. These resonance patterns reflect helical wheels and the position, size, and shape of the pattern reflects the tilt of the helical axis with respect to the bilayer normal.[30] In fitting PISA wheels to experimental spectra, the PISA wheels are rigidly constrained by the spin interaction tensor element magnitudes and their relative orientation. The only variable is the helical tilt and this is fit by eye to the experimental data generating an estimate of the helical tilt that has an error of not more than $\pm 3^\circ$ when the tilt angles are greater than 10°. These initial estimates of tilt before resonance assignments have been made provide useful preliminary structural insights. Following resonance assignments, a high-resolution structure can be characterized from the PISEMA structural restraints.

Figure 5 shows the influence of random variations in ϕ and ψ torsion angles on the potential observation of PISA wheels. There are several factors that can disperse the resonances of the helical backbone, potentially blurring or eliminating the observation of such a wheel-like pattern. Chemical shift tensors can vary, especially those associated with glycine are significantly different[61] from other residues, and because the amide nitrogen of proline is not protonated such resonances are not observed in the PISA wheels. The relative orientation of the ^{15}N-chemical shift tensor and the ^{15}N–^{1}H dipolar interaction may differ from site to site. These factors have been discussed in some detail in the literature,[30,45,62,63] and their influence on the dispersion of resonances is relatively small. For example, the angle between the ^{15}N chemical shift tensor and ^{15}N–^{1}H bond vector varies only by 2° on an average for nonglycine residues based on *ab initio* calculations[64] and even less in an experimental study of a membrane bound peptide.[61] Starting from the ideal values for an 18-residue TM helix ($\phi = -60^\circ$, $\psi = -45^\circ$)[38] tilted at 30° with respect to the

DOI: 10.1002/mrc

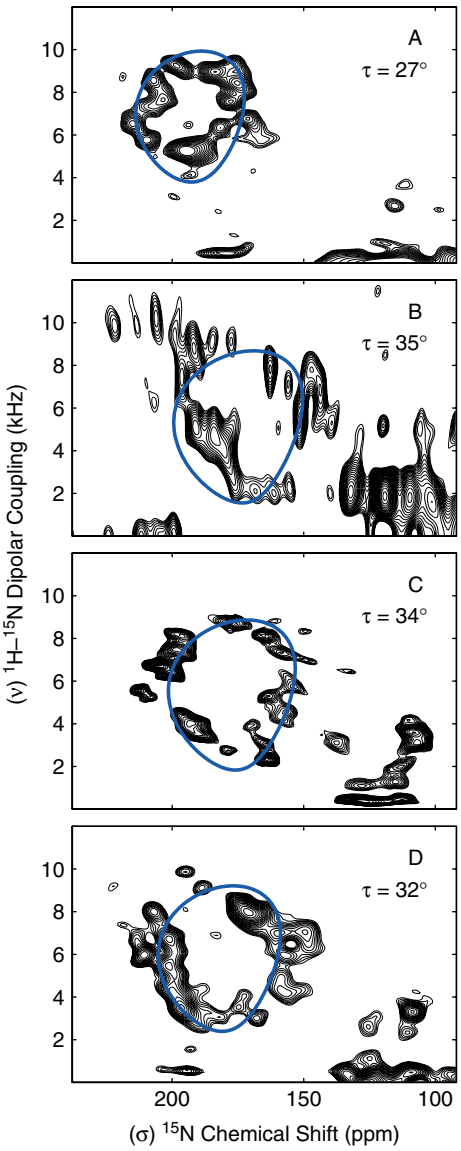

Figure 4. PISEMA spectra of CorA-TM2 (A), KdpC-TM (B), KdpF (C), and M2-TMD (D) are indicative of highly regular helical structures. The helix axis tilt angle (τ) with respect to the bilayer normal and corresponding PISA wheel (blue) is shown for the spectrum of each transmembrane peptide. All the spectra were acquired with uniformly ^{15}N-labeled peptides in DMPC/DMPG lipid bilayers oriented on glass slides.

bilayer normal, PISEMA spectra were simulated (Fig. 5(A)). Additional simulations varied these torsion angles within $\pm 2^\circ$, 4°, 8°, and 16° for Figs 5(B–E) respectively. The resulting random dispersion of torsion angles is illustrated with the Ramachandran diagram beside each spectral simulation. The PISA wheel pattern essentially disappears when the torsion angles have a variation within $\pm 8^\circ$ (Fig. 5(D)). The observed PISA wheels in Fig. 4 suggest that if all the dispersion in the chemical shift and dipolar dimensions is due to this structural variation, then for these peptides the variation in ϕ,ψ torsion angles is approximately $\pm 4^\circ$. Since we know that the chemical shift tensor variations are significant, this observed structural variation is a maximum value that, in reality, is likely to be less than $\pm 4^\circ$. Such a small variation in angle means that a PISA wheel is observed only when the helix has a remarkably uniform structure.

The TM helix–helix interface

Interestingly, M2-TMD that generates one of the PISA wheels in Fig. 4 forms a tetrameric complex. Despite these asymmetric interhelical interactions, each helix retains a very uniform structure and shows no evidence of a coiled-coil structure.[62] In part, owing to the limited electrostatic potential of most TM amino acid residues and in part to the environment provided by the lipid bilayer, the interhelical molecular interactions are dominated by van

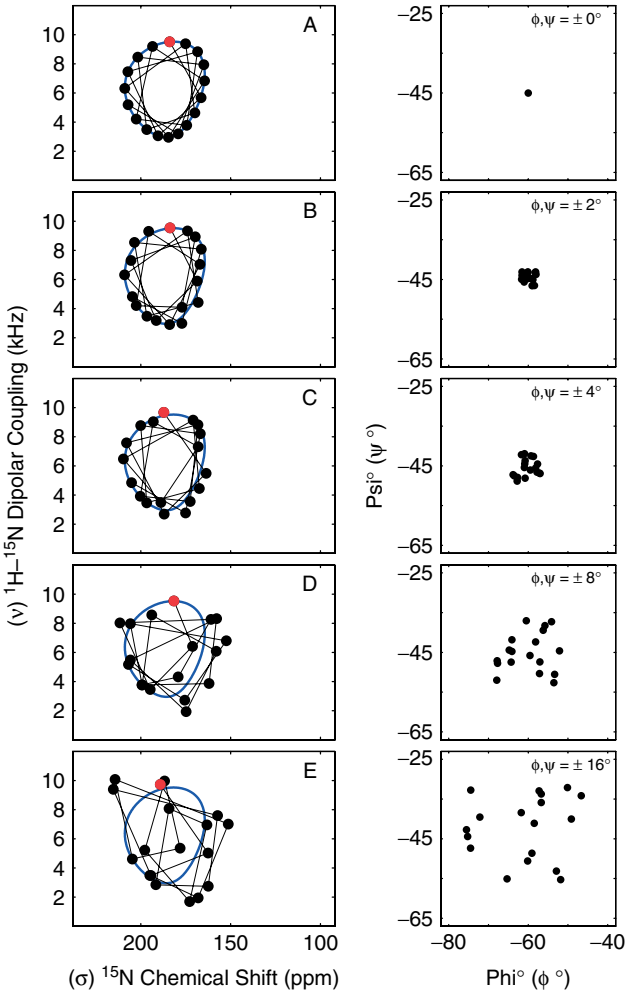

Figure 5. The sensitivity of PISEMA spectra to changes in backbone ϕ,ψ torsion angles is illustrated through spectral simulations of an 18-residue helical peptide with a helix axis tilt angle (τ) of 30° with respect to the bilayer normal. Displayed for each simulated PISEMA spectrum are a PISA wheel with $\tau = 30^\circ$ (blue line), location of the starting residue (red dot), location of resonances 2 through 18 (black dots) and the sequential trace of resonances (thin black line). Initial simulations were performed for an ideal α-helix ($\phi = -60^\circ$, $\psi = -45^\circ$)[38] (A). ϕ,ψ torsion angles for each residue were then allowed to vary randomly from the ideal values by $\pm 2^\circ$ (B), $\pm 4^\circ$ (C), $\pm 8^\circ$ (D), and $\pm 16^\circ$ (E). A Ramachandran plot centered on the α-helical region shows the distribution of ϕ,ψ torsion angles for the resonances in each simulation.

DOI: 10.1002/mrc

der Waals interactions. Since these latter interactions are nonspecific, there are likely to be multiple low energy solutions. As mentioned earlier, the full-length M2 protein appears to display large amplitude rotational excursions about the helical axis as characterized from H/D exchange experiments.[9] In addition, it has been shown that the tilt of the M2 helices in M2-TMD are highly dependent on the fatty acyl chain length.[65] Both of these results support the hypothesis that nonspecific van der Waals interactions are dominating the helical interface.

Recent literature for M2-TMD has also exemplified another feature of its sequence. While we have shown that uniform helices can be formed with proline and glycine residues present, they retain their potential to kink helices. In the presence of the antiviral drug, amantadine, the M2-TMD helix is kinked in the vicinity of its glycine residue.[46] Other examples of functionally relevant conformational switches that have been described in the literature are centered on glycine or proline residues, such as the opening and closing of the potassium channel KcsA.[66] Consequently, when these residues are part of a uniform helical structure they can be thought of as 'pro-kink' sites.

Figure 6 illustrates the dependence of the CorA-TM2 peptide on its lipid environment through the recording of PISEMA spectra in both DMPC/DMPG and POPC/POPG lipid bilayers. Clearly, the helical tilt of CorA-TM2 is dependent on the hydrophobic thickness of the bilayer and hence, we would argue that again the interactions of the helical interface are dominated by nonspecific van der Waals interactions. However, in Fig. 6 we also show data for ^{15}N-methionine labeled DAGK, a protein with three TM helices that functions as a trimer. While the quality of the aligned spectra varies (more or less powder pattern present), the frequency of the resonance representing the aligned sample does not change with increasing hydrophobic thickness of the lipid bilayers. Consequently, specific interactions must be present to have locked this conformation in, preventing the potential for hydrophobic mismatch to alter the protein structure. In part, this is the result of mutagenesis.[48] There are several ways in which hydrophobic mismatch can be compensated for, as reviewed recently by Killian and Nyholm.[67] Here, two examples are presented, one (CorA-TM2) where the helical tilt changes and another (DAGK) where the specific interactions appear in this 9-helix bundle to have locked in a specific conformation, preventing changes in helical tilt in response to changes in bilayer thickness.

Hydrogen-bonding and electrostatic interaction capacity, while much less frequent in TM helical interfaces, is still present in some membrane proteins. Such capacity is achieved in several ways. Small residues such as glycine, alanine, and serine are sometimes spaced to be on one side of a helix such as GxxxG and GxxxxxG (known as GG4 and GG7) to permit close packing of helices.[13,14,68,69] Such packing allows for potential C_α–H···O hydrogen bonding[70,71] as well as long distance, but significant, electrostatic interactions between the polypeptide backbones. Alternatively, serine and threonine residues are more common in the membrane interstices than might be expected because of their ability to form intrahelical hydrogen bonds. Such residues also have the potential to form interhelical hydrogen bonds and can therefore be considered 'pro-hydrogen bond' residues. A third mechanism for specific electrostatic interactions involves a relatively small separation of charged residues in the TM sequence resulting in the demand for pairing charges to obtain a stable structure.

For CorA-TM2, there is a single GG7 sequence with a valine in the center of the sequence. This valine residue,

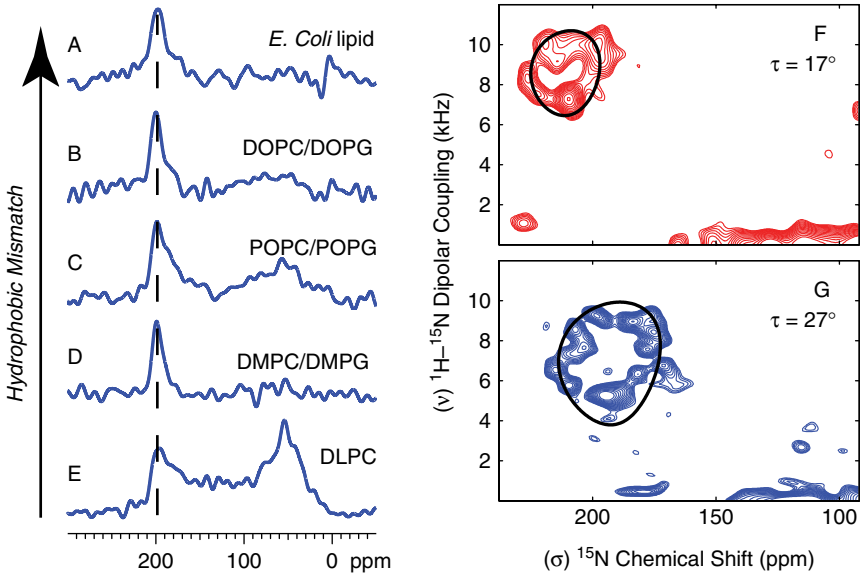

Figure 6. The response of proteins and peptides to changes in lipid bilayer hydrophobic thickness varies depending on the types and strengths of interactions present. The location of resonances for ^{15}N-methionine labeled DAGK undergo very little change as the hydrophobic thickness of the bilayer increases, indicating very little change in overall structure. This is shown for one-dimensional ^{15}N-spectra acquired in lipid bilayers composed of *E. Coli* lipid (A), DOPC/DOPG (B), POPC,POPG (C), DMPC/DMPG (D), and DLPC (E). Conversely, PISEMA spectra of uniformly ^{15}N-labeled CorA-TM2 indicate a 10° change in helix axis tilt angle (τ) in response to an increased hydrophobic thickness for POPC/POPG lipid bilayers (F) compared to DMPC/DMPG lipid bilayers (G).

DOI: 10.1002/mrc

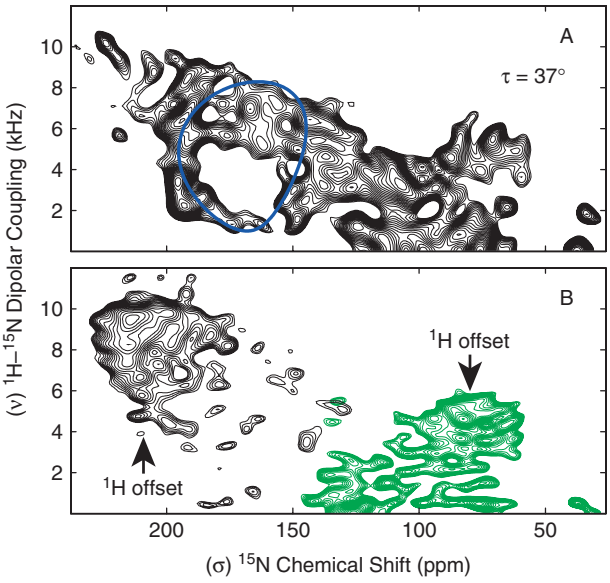

Figure 7. PISEMA spectra are shown for the full-length membrane proteins Rv1861 (A) and DAGK (B). Rv1861 demonstrates a clear PISA wheel pattern with a helix axis tilt angle (τ) of 37°. Resonances for DAGK are tightly clustered in the 200 ppm and 8 kHz region indicating small helix tilt angles for the three TM helices in DAGK. Spectra for DAGK were collected using two separate experiments with different ^{1}H offset positions to avoid ^{1}H bandwidth limitations. Both Rv1861 and DAGK spectra were acquired with uniformly ^{15}N-labeled protein in DMPC/DMPG lipid bilayers oriented on glass slides.

with a beta-branched side chain, would likely interfere with close packing of helices. It is therefore not surprising that this peptide is monmeric and that the helical tilt is very sensitive to the bilayer hydrophobic thickness. For DAGK, the hydrophobic cores of the TM helices are relatively short. For the three helices, 14, 13, and 11 residues separate two charged residues, although for TM3 this is the result of the stabilizing mutation V107D. In comparison, all of the other sequences in Fig. 3 have at least 18 residues separating charged residues with the exception of the functionally conserved histidine residue in M2 which has unique properties as a histidine tetrad.[72] This suggests that electrostatic interactions between the ends of adjacent TM helices of DAGK are very significant.

Figure 7 displays PISEMA spectra of two full-length proteins, one of which, Rv1861, shows a PISA wheel pattern. This observation, not only means that uniform helical structures are present, but confirms the previous discussions on the altered balance of molecular interactions that result in such uniform helices. There has been discussion in the literature that PISA wheels may not be observable for native proteins, because the helices might have nonideal conformations.[73] It is now clear that full-length membrane protein TM helices can have very uniform torsion angles, although this will certainly not be true for all the TM helices. Despite the large 80 kDa oligomeric complex for Rv1861 with 24 TM helices, the interstices of the TM domain

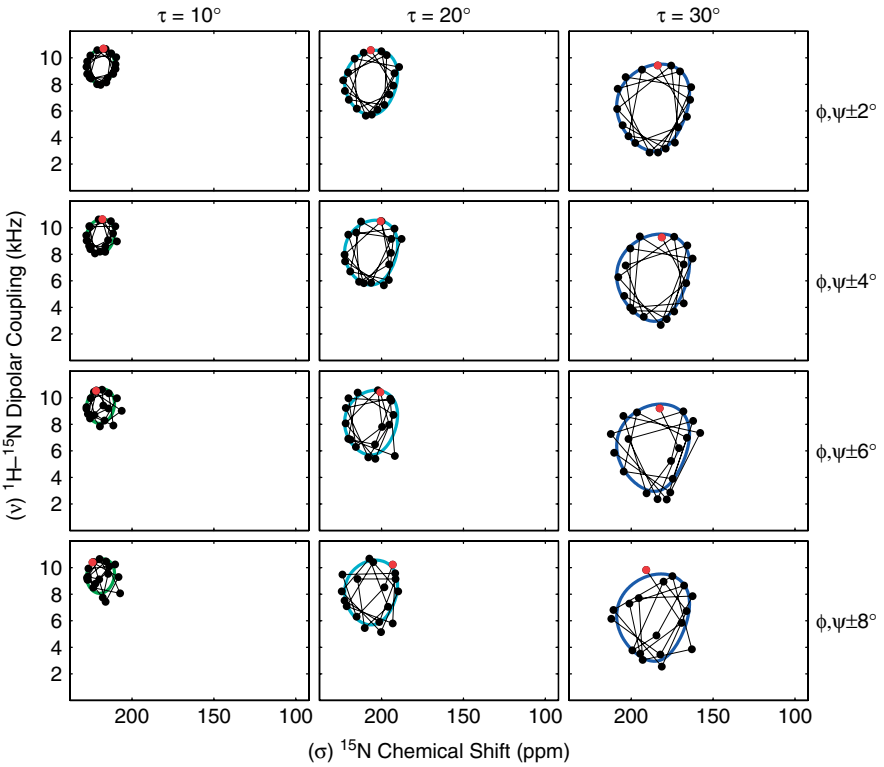

Figure 8. Spectral simulations of an 18-residue α-helical peptide illustrate that changes in PISEMA spectra owing to variations in ϕ,ψ torsion angles are scaled down as the helix axis tilt angle (τ) decreases. PISEMA spectra for three α-helical peptides with $\tau = 10°$, 20°, and 30° were simulated with ϕ,ψ torsion angles for each residue allowed to vary randomly from the ideal values ($\phi = -60°$, $\psi = -45°$)[38] by ±2°, ±4°, ±6°, and ±8° as indicated. For each simulated PISEMA spectrum, a PISA wheel (green, cyan, and blue lines for $\tau = 10°$, 20°, and 30° respectively), location of the starting residue (red dot), locations of resonances 2 through 18 (black dots) and the sequential trace of resonances (thin black line) are shown.

DOI: 10.1002/mrc

still reflect the typical membrane environment where the balance of molecular interactions is so very different from water-soluble proteins. DAGK is also well aligned in planar bilayers, but PISA wheels were not observed in the spectra of uniformly ^{15}N-labeled samples. DAGK is a trimer of three TM helical monomer with relatively small water-soluble loops and terminal segments. Even though PISA wheels were not obtained, the spectral intensity from the TM domain is tightly clustered in a region around 200 ppm and 8 kHz suggesting small tilt angles for the TM helices. From the spectra of ^{15}N-methionine labeled DAGK, it has recently been suggested that one of the helices is tilted by $12 \pm 3°$.[45]

Figure 8 shows spectral simulations similar to those shown in Fig. 5, but with varying helical tilt angle. Interestingly, the dispersion caused by ϕ,ψ torsion angle variation scales with decreasing helical tilt angles. Consequently, while it might have been anticipated that a structurally induced dispersion in chemical shift of 10 ppm for a helix tilted at 30° would obliterate the PISA wheel for a helix tilted at 10°; the scaling by this effect is such that the PISA wheels are nearly as clear for a 10° helical tilt as they are for a 30° tilt with the same ϕ,ψ torsion angle variation. However, other influences on the dispersion of the resonances, such as the variation in the chemical shift tensor do not scale in the same manner. The spectrum of CorA-TM2 is particularly interesting in this regard as the pattern of resonances with its various defects are highly correlated for the two different tilt angles in Fig. 6(F) and (G) Yet, the hole in the spectral intensity at the center of the PISA wheel is substantially smaller than would be estimated just from the size of the wheels, suggesting that the dispersion has not been fully scaled and that some of the dispersion in the POPC/POPG sample may be from the variation in chemical shift tensors. Similarly, with the spectral congestion in the 200 ppm region of the DAGK spectrum, resonance patterns are simply not observable because of factors other than the variation in ϕ,ψ torsion angles.

CONCLUSIONS

A dramatic shift in the balance of molecular interactions for membrane proteins with respect to soluble proteins is evidenced by the uniform helical structures that are repeatedly being characterized by solid-state NMR of TM helical peptides as well as full-length membrane proteins. The implications for this shift in balance are profound. Membrane protein environments interact with membrane proteins in a spatially selective manner. Van der Waals interactions will dominate the environment/protein interface in the bilayer interstices while electrostatic interactions are more important in the lipid/protein interfacial and aqueous regions. Physical properties of the bilayer may change in response to environmental stress on the cell and the chemical composition of the membranes may change as well, each leading to potential changes in the membrane/protein interfacial interactions. The relatively weak interactions that may be present between helices make possible a wide range of structural conformations that are being shown to have functional importance. Therefore, the challenge for the membrane protein structural biologist is not the characterization of structure for a membrane protein, but to characterize a potential energy surface and a suite of structures reflecting the subtle influences of the environment. Consequently, it is very important to characterize membrane proteins in an environment that closely models the native membrane environment. Solid-state NMR can provide the most native-like environment for the detailed characterizations of membrane proteins and has great potential for characterizing membrane proteins under a wide range of environmental conditions.

Acknowledgements

This work was supported by NIH grants PO1 GM-67476 and RO1 AI23007. R.C. Page was supported by American Heart Association predoctoral fellowship 0615223B. The authors are grateful to C. Sanders for providing the DAGK plasmid and protocol for DAGK purification. Experiments were conducted at the National High Field Magnetic Laboratory, supported by cooperative Agreement (Grant DMR-0084173) and the State of Florida.

REFERENCES

1. London E. *Curr. Opin. Struct. Biol.* 2002; **12**: 480.
2. White SH, Wiener MC. In *Permeability and Stability of Lipid Bilayers*, Disalvo EA, Simon SA (eds). CRC Press: Boca Raton, 1994; 1.
3. Marrink S-J, Berkowitz M. In *Permeability and Stability of Lipid Bilayers*, Disalvo EA, Simon SA (eds). CRC Press: Boca Raton, 1994; 21.
4. Cantor RS. *Biophys. J.* 1999; **76**: 2625.
5. Botelho AV, Gibson NJ, Thurmond RL, Wang Y, Brown MF. *Biochemistry* 2002; **41**: 6354.
6. Sachs JN, Engelman DM. *Annu. Rev. Biochem.* 2006; **75**: 707.
7. Eilers M, Patel AB, Liu W, Smith SO. *Biophys. J.* 2002; **82**: 2720.
8. Hunt JF, Earnest TN, Bousche O, Kalghatgi K, Reilly K, Horvath C, Rothschild KJ, Engelman DM. *Biochemistry* 1997; **36**: 15156.
9. Tian C, Gao PF, Pinto LH, Lamb RA, Cross TA. *Protein Sci.* 2003; **12**: 2597.
10. Nagy JK, Lonzer WL, Sanders CR. *Biochemistry* 2001; **40**: 8971.
11. Hwang PM, Choy WY, Lo EI, Chen L, Forman-Kay JD, Raetz CR, Prive GG, Bishop RE, Kay LE. *Proc. Natl. Acad. Sci. U.S.A.* 2002; **99**: 13560.
12. Spencer RH, Rees DC. *Annu. Rev. Biophys. Biomol. Struct.* 2002; **31**: 207.
13. MacKenzie KR, Prestegard JH, Engelman DM. *Science* 1997; **276**: 131.
14. Javadpour MM, Eilers M, Groesbeek M, Smith SO. *Biophys. J.* 1999; **77**: 1609.
15. Arumugam S, Pascal S, North CL, Hu W, Lee KC, Cotten M, Ketchem RR, Xu F, Brenneman M, Kovacs F, Tian F, Wang A, Huo S, Cross TA. *Proc. Natl. Acad. Sci. U.S.A.* 1996; **93**: 5872.
16. Popot JL, Engelman DM. *Biochemistry* 1990; **29**: 4031.
17. Engelman DM. *Science* 1996; **274**: 1850.
18. Im W, Brooks CL III. *Proc. Natl. Acad. Sci. U.S.A.* 2005; **102**: 6771.
19. Sheinerman FB, Brooks CL III. *Proc. Natl. Acad. Sci. U.S.A.* 1998; **95**: 1562.
20. Robinson GW, Cho CH. *Biophys. J.* 1999; **77**: 3311.
21. Fitter J. *Biophys. J.* 1999; **76**: 1034.
22. Xu F, Cross TA. *Proc. Natl. Acad. Sci. U.S.A.* 1999; **96**: 9057.
23. Patzlaff JS, Moeller JA, Barry BA, Brooker RJ. *Biochemistry* 1998; **37**: 15363.
24. Oxenoid K, Kim HJ, Jacob J, Sonnichsen FD, Sanders CR. *J. Am. Chem. Soc.* 2004; **126**: 5048.
25. Chekmenev EY, Gor'kov PL, Cross TA, Alaouie AM, Smirnov AI. *Biophys. J.* 2006; **91**: 3076.
26. Li C, Mo Y, Hu J, Chekmenev E, Tian C, Gao FP, Fu R, Gor'kov P, Brey W, Cross TA. *J. Magn. Reson.* 2006; **180**: 51.
27. Gor'kov PL, Chekmenev EY, Li C, Cotten M, Buffy JJ, Traaseth NJ, Veglia G, Brey WW. *J. Magn. Reson.* 2007; **185**: 77.

28. Wu CH, Ramamoorthy A, Opella SJ. *J. Magn. Reson., Ser. A* 1994; **109**: 270.
29. Ramamoorthy A, Wei Y, Lee D-K, Webb GA. In *Annual Reports on NMR Spectroscopy*, vol. 52, Webb GA (ed). Academic Press: 2004; 1.
30. Wang J, Denny J, Tian C, Kim S, Mo Y, Kovacs F, Song Z, Nishimura K, Gan Z, Fu R, Quine JR, Cross TA. *J. Magn. Reson.* 2000; **144**: 162.
31. Marassi FM, Opella SJ. *J. Magn. Reson.* 2000; **144**: 150.
32. Bracy DS, Schenerman MA, Kilberg MS. *Biochim. Biophys. Acta* 1987; **899**: 51.
33. Marassi FM, Crowell KJ. *J. Magn. Reson.* 2003; **161**: 64.
34. Rainey JK, Sykes BD. *Biophys. J.* 2005; **89**: 2792.
35. Fung BM, Khitrin AK, Ermolaev K. *J. Magn. Reson.* 2000; **142**: 97.
36. Delaglio F, Grzesiek S, Vuister GW, Zhu G, Pfeifer J, Bax A. *J. Biomol. NMR* 1995; **6**: 277.
37. Goddard T, Kneller D. *Sparky 3*. University of California: San Francisco.
38. Kim S, Cross TA. *Biophys. J.* 2002; **83**: 2084.
39. Teng Q, Iqbal M, Cross TA. *J. Am. Chem. Soc.* 1992; **114**: 5312.
40. Bowie JU. *Nature* 2005; **438**: 581.
41. Wimley WC, White SH. *Nat. Struct. Biol.* 1996; **3**: 842.
42. White SH, von Heijne G. *Curr. Opin. Struct. Biol.* 2005; **15**: 378.
43. Lunin VV, Dobrovetsky E, Khutoreskaya G, Zhang R, Joachimiak A, Doyle DA, Bochkarev A, Maguire ME, Edwards AM, Koth CM. *Nature* 2006; **440**: 833.
44. Laimins LA, Rhoads DB, Altendorf K, Epstein W. *Proc. Natl. Acad. Sci. U.S.A.* 1978; **75**: 3216.
45. Li C, Gao P, Qin H, Chase R, Gor'kov PL, Brey WW, Cross TA. *J. Am. Chem. Soc.* 2007; **129**: 5304.
46. Hu J, Asbury T, Achuthan S, Li C, Bertram R, Quine JR, Fu R, Cross TA. *Biophys. J.* 2007; **92**: 4335.
47. Nishimura K, Kim S, Zhang L, Cross TA. *Biochemistry* 2002; **41**: 13170.
48. Zhou Y, Bowie JU. *J. Biol. Chem.* 2000; **275**: 6975.
49. Luecke H, Schobert B, Richter HT, Cartailler JP, Lanyi JK. *J. Mol. Biol.* 1999; **291**: 899.
50. Baker EN, Hubbard RE. *Prog. Biophys. Mol. Biol.* 1984; **44**: 97.
51. Ketchem RR, Lee KC, Huo S, Cross TA. *J. Biomol. NMR* 1996; **8**: 1.
52. Prosser RS, Hunt SA, Vold RR. *J. Magn. Reson., Ser. B* 1995; **109**: 109.
53. Marassi FM, Opella SJ. *Curr. Opin. Struct. Biol.* 1998; **8**: 640.
54. Marassi FM, Opella SJ. *Protein Sci.* 2003; **12**: 403.
55. De Angelis AA, Howell SC, Nevzorov AA, Opella SJ. *J. Am. Chem. Soc.* 2006; **128**: 12256.
56. Lu JX, Damodaran K, Lorigan GA. *J. Magn. Reson.* 2006; **178**: 283.
57. Park SH, De Angelis AA, Nevzorov AA, Wu CH, Opella SJ. *Biophys. J.* 2006; **91**: 3032.
58. Durr UH, Yamamoto K, Im SC, Waskell L, Ramamoorthy A. *J. Am. Chem. Soc.* 2007; **129**: 6670.
59. Lorigan GA, Dave PC, Tiburu EK, Damodaran K, Abu-Baker S, Karp ES, Gibbons WJ, Minto RE. *J. Am. Chem. Soc.* 2004; **126**: 9504.
60. Chekmenev EY, Hu J, Gor'kov PL, Brey WW, Cross TA, Ruuge A, Smirnov AI. *J. Magn. Reson.* 2005; **173**: 322.
61. Mai W, Hu W, Wang C, Cross TA. *Protein Sci.* 1993; **2**: 532.
62. Wang J, Kim S, Kovacs F, Cross TA. *Protein Sci.* 2001; **10**: 2241.
63. Poon A, Birn J, Ramamoorthy A. *J. Phys. Chem. B* 2004; **108**: 16577.
64. Brender JR, Taylor DM, Ramamoorthy A. *J. Am. Chem. Soc.* 2001; **123**: 914.
65. Duong-Ly KC, Nanda V, Degrado WF, Howard KP. *Protein Sci.* 2005; **14**: 856.
66. Cordero-Morales JF, Cuello LG, Zhao Y, Jogini V, Cortes DM, Roux B, Perozo E. *Nat. Struct. Mol. Biol.* 2006; **13**: 311.
67. Killian JA, Nyholm TK. *Curr. Opin. Struct. Biol.* 2006; **16**: 473.
68. Senes A, Gerstein M, Engelman DM. *J. Mol. Biol.* 2000; **296**: 921.
69. Liu Y, Engelman DM, Gerstein M. *Genome Biol.* 2002; **3**: research0054.1.
70. Senes A, Ubarretxena-Belandia I, Engelman DM. *Proc. Natl. Acad. Sci. U.S.A.* 2001; **98**: 9056.
71. Curran AR, Engelman DM. *Curr. Opin. Struct. Biol.* 2003; **13**: 412.
72. Hu J, Fu R, Nishimura K, Zhang L, Zhou HX, Busath DD, Vijayvergiya V, Cross TA. *Proc. Natl. Acad. Sci. U.S.A.* 2006; **103**: 6865.
73. Straus SK, Scott WR, Watts A. *J. Biomol. NMR* 2003; **26**: 283.

DOI: 10.1002/mrc